Analysis of transport barriers with the oscillatory state for plasma dynamics in helical plasmas

S. Toda[1], K. Itoh[1] and A. Wakasa[2]

[1]*National Institute for Fusion Science, Toki 509-5292, Japan*

[2]*Department of Nuclear Engineering, Kyoto University, Sakyo-ku, Kyoto 606-8501, Japan*

1. Introduction

The formation mechanism of transport barriers is important issue to realize improved confinement modes in toroidal plasmas. The profile of the radial electric field is known to strongly affect the confinement property, which is related with the transport barrier, in toroidal plasmas. In the nonaxisymmetric system, the radial electric field is determined by the ambipolar condition [1]. The limit cycle phenomena in the temporal evolution of the electrostatic potential between two states, namely the electric pulsation, have been observed in Compact Helical System (CHS) [2] and Large Helical Device (LHD) [3]. The further calculation for the neoclassical flux which includes the detailed magnetic configuration and applicable to the wide collisional region is needed to accurately predict the parameter region for the self-generated oscillation of E_r in the LHD, because the neoclassical transport strongly affects the turbulent transport due to the profile of E_r in helical plasmas. In our previous work, temporally oscillatory state of the radial electric field has been obtained [4]. A neoclassical transport database DCOM/NNW for LHD (DGN/LHD) has been constructed [5]. To theoretically predict the electric pulsation in the core region of helical plasmas, the transport model for LHD-like plasmas is constituted by the one-dimensional diffusion equations of the density, the electron and ion temperatures, and the radial electric field. In order to estimate the neoclassical transport and the ambipolar radial electric field for LHD in details, the DGN/LHD for the nonaxisymmetric part of the radial flux is adopted in the diffusive equations. The DGN/LHD is used for the simulation to reproduce the electric pulsation and to predict the parameter region for the electric pulsation in the LHD experimental results. The dependence of the transition point for the radial electric field on the particle source is studied. The variation of the solution type (the stationary or oscillatory state) is also examined.

2. One-dimensional transport model

The one-dimensional transport equations used here are same as those shown in [4]. In this study, the DGN/LHD is used for the nonaxisymmetric part of the radial neoclassical flux in the diffusion equations. The diffusion coefficient in the DGN/LHD is given by the multi-helicity model [6]. The DGN/LHD includes the detailed magnetic configuration properties. This database is applicable to the wide collision regime from $1/\nu_j$ regime to Pfirsh-Schlüter regime, where ν_j is the collision frequency of species j. In the previous paper [4], the analytic formula [7] was used for the neoclassical flux, which covers from the ν_j regime to the $1/\nu_j$ regime. This analytic formula assumes a model magnetic field with a single helicity, which strongly limits its rigorous applicability for wide range equilibria in LHD. However, by em-

ploying such an analytical formula, it is predicted that the self-generated oscillation takes place from some physical mechanism related with the flux-gradient relation [4]. We adopt the model for the anomalous heat diffusivity based on the theory of the self-sustained turbulence due to the interchange mode, driven by the current diffusivity [8] as a candidate. The value for the anomalous diffusivities of the particle is chosen $D_a = 1\mathrm{m}^2\mathrm{s}^{-1}$, which is set to be constant spatially and temporally. The value of the diffusion coefficient for the radial electric field D_{Ea} is set as $D_{Ea} = 1\mathrm{m}^2/\mathrm{s}$. Throughout this article, the heating source of electrons and ions is set to be proportional to the relation $\exp(-(r/(0.3a))^2)$, which corresponds to the central heating experimentally, *e.g.*, the ECRH. The particle source S_n is set to be $S_n = S_0 \exp((r-a)/L_0)$, where L_0 is set to be 0.03m. We employ the same boundary conditions at the center of the plasma ($\rho = 0$) and at the edge ($\rho = 1$) as those in [4], where $\rho = r/a$. The machine parameters are similar to those of LHD, such as the major radius $R = 3.6$m, $a = 0.6$m and the toroidal magnetic field $B = 2.85$T. In this case, we set the safety factor as $q = 1/(1+(r/a)^2)$.

3. Results of the analysis

The one-dimensional transport analysis for the LHD-like plasma has been performed and the profiles of n, T_e, T_i and E_r are solved as the initial value problem. The self-generated oscillation in a limited region of the parameter space is examined near the transition layer between the positive E_r and the negative E_r due to the multiple ambipolar E_r in the core plasma region. The absorbed power of electrons is set to be 1MW and the coefficient S_0 is taken as $5.31 \times 10^{21}\mathrm{m}^{-3}\mathrm{s}^{-1}$. The absorbed power of ions is taken as 300kW. The temporal evolution in the time interval $0.98\mathrm{s} \leq \mathrm{t} \leq 1.00\mathrm{s}$ of the radial electric field, E_r is plotted in Fig. 1. The lines labeled by $\rho = 0.1$, $\rho = 0.2$, $\rho = 0.3$, $\rho = 0.5$ and $\rho = 1.0$ show the temporal evolutions of E_r, respectively. The state A at $t = 0.9846$s indicates the one at $\rho = 0.1$ just after the transition from the negative E_r to the positive E_r in Fig. 1. From the state A, the plasma profile changes with the transport time scale and reaches the state B at $t = 0.9860$s. Just after the transition from the state B, the state changes to the one C at $t = 0.9862$s. From the state C, the plasma state changes to the state D at $t = 0.9886$s with the transport time scale. Just after the state D, the transition from the negative E_r to the positive E_r takes place at $\rho = 0.1$ and the state comes back to the one A at $t = 0.9888$s. The temporal evolutions in the core region (at $\rho = 0.1$ and $\rho = 0.2$) clearly show the characteristic of the limit cycle. In the core region at $\rho = 0.1$, the transitions occur from the negative E_r to the positive E_r at $t = 0.9844$s and from the positive E_r to the negative E_r at $t = 0.9860$s in Fig. 1. The time period of the limit cycle is about 5ms, which is determined by the typical transport time scale. The self-generated oscillation of the radial electric field is shown to have

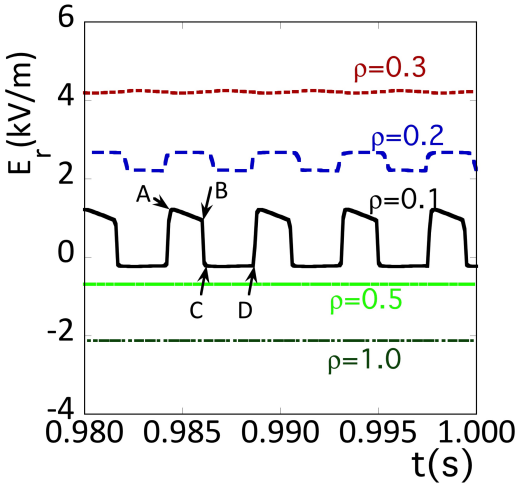

Figure 1: The self-generated oscillation for the radial electric field in the core region.

two time scales: a slow time scale of the transport and a fast time scale at the transition. The temporal change of the E_r profile causes the temporal change of the radial profile of the neoclassical and anomalous diffusivities. Owing to the influence of E_r on transport coefficients, the temporal evolution of the radial T_e, T_i and n profiles takes place as the limit cycle in the core region.

We plot the temporal change of the profiles of E_r in Fig. 2(a) at the states A and C. At both states A and C, the radial transition at the radial point ρ_T, where the parameter ρ_T is the radial location of the transition point from the positive E_r to the negative E_r. At the state C, the radial transition from the negative E_r to the positive one takes place around $\rho = 0.1$ due to the multiple radial electric field for the ambipolar condition in Fig. 2(a). The radial profiles of the electron heat diffusivity χ_e^{NEO} with the solid line, the ion neoclassical heat diffusivity χ_i^{NEO} with the dashed line and the anomalous heat diffusivity χ_a with the dotted line at the state A are shown in Fig. 2(b). The diffusivities χ_e^{NEO} and χ_i^{NEO} represent $-Q_e^{NEO}/T_e'$ and $-Q_i^{NEO}/T_i'$, where the prime denotes the radial derivative. The symbols Q_e^{NEO} and Q_i^{NEO} represent the electron and ion neoclassical heat flux. Because of the shear of the radial electric field at ρ_T, the reduction of the anomalous heat diffusivity is found around $\rho = \rho_T$ in Fig. 2(b). At the state A, the reduction of the neoclassical transport is also shown in the wide region $\rho < \rho_T$.

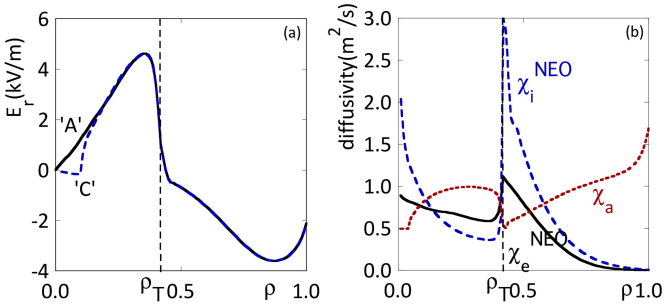

Figure 2: (a) The radial profiles of the electric field at the states A and C. (b) The radial profiles of χ_e^{NEO}, χ_i^{NEO} and χ_a at the state A.

We examine the dependence of the transition point ρ_T on the particle source S_0. The values of other parameters except the particle source are same as the analysis done before in this study. When the particle source is $S_0 = 1.0 \times 10^{21}\mathrm{m}^{-3}\mathrm{s}^{-1}(\bar{\mathrm{n}} = 1.99 \times 10^{18}\mathrm{m}^{-3})$, the multiple solutions of E_r for the ambipolar condition are found, where the quantity with the bar represents the line-averaged value. The positive E_r in the core region, the negative E_r in the edge region and the radial transition of E_r at $\rho_T = 0.90$ are shown in a stationary state. If the value of the particle source S_0 increases, the transition point ρ_T moves inside shown in Fig. 3. In Fig. 3, the open circles show the stationary state. In the case of the closed circles, the self-generated oscillation takes place around $\rho = 0.1$ explained before in this study. When the line-averaged density $\bar{n}$ increases further and becomes larger than $1.2 \times 10^{19}\mathrm{m}^{-3}$, the radial electric field takes the negative value in the radial entire

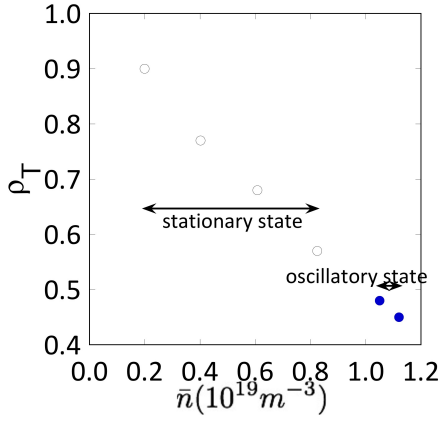

Figure 3: The dependence of the transition point ρ_T location on the line-averaged density $\bar{n}$

region.

We study the conditions in the parameter space, where the self-generated oscillation occurs. When the intensity of source is varied, the mean values of the n, T_e and T_i change, and the temporal evolution of calculations reaches either the stationary state or the self-generated oscillation. The parameter regime for the multiple solutions of the ambipolar E_r at a radial point is examined. In this region, the so-called 'hard' transition occurs between the multiple ambipolar E_r. The region for the self-generated oscillation is shown: $1 < \bar{T}_e/\bar{T}_i < 3$ and $\bar{n} \approx 1 \times 10^{19}\mathrm{m}^{-3}$, using the DGN/LHD database for the neoclassical diffusion coefficient. In the previous study where the analytic formula [7] was used, the region for the self-generated oscillation was shown: $1 < \bar{T}_e/\bar{T}_i < 2$ and $\bar{n} \approx 1 \times 10^{19}\mathrm{m}^{-3}$[4]. The larger value of $\bar{T}_e/\bar{T}_i$ is predicted for the self-generated oscillation when the DGN/LHD is used compared with the analysis when the analytic formula is adopted. The region for the self-generated oscillation is inside the region for the multiple E_r of the ambipolar condition. The physical mechanism to realize a self-generated oscillation was studied, which relates the flux-gradient relation with the hysteresis characteristic [4].

4. Summary

In this study, the DGN/LHD database for the neoclassical transport coefficients related with helical-ripple trapped particles is included in a set of one-dimensional transport equations. The self-generated oscillation of the radial electric field in the core region is shown. The dependence of the location of the radial transition point for the electric field on the particle source is studied, when the plasma state changes from the stationary state to the oscillatory state. The parameter regime for the self-generated oscillation is shown: $1 < \bar{T}_e/\bar{T}_i < 3$ and $\bar{n} \approx 1 \times 10^{19}\mathrm{m}^{-3}$ on $\bar{T}_e/\bar{T}_i - \bar{n}$ plane, when the DGN/LHD database is used for the neoclassical transport coefficients. This result agrees with the experimental result that the electric field pulsation is observed in the low density ($\bar{n} \approx 0.5 \times 10^{19}\mathrm{m}^{-3}$) and the high electron temperature ($1 < \bar{T}_e/\bar{T}_i < 3$) in LHD plasmas [3].

Acknowledgements

This work was partly supported by Grant-in-Aid for Scientific Research of JSPS (23561002 and 23244113).

References

[1] H. Sugama, T. -H. Watanabe, M. Nunami and S. Nishimura, Plasma Phys. Control. Fusion **53** (2011) 024004

[2] A. Fujisawa *et al.*, Phys. Rev. Lett. **81** (1998) 2256

[3] A. Shimizu *et al.*, Plasma Fusion Research **5** (2010) S1015

[4] S. Toda and K. Itoh, Plasma Phys. Control. Fusion **53** (2011) 115011

[5] A. Wakasa, S. Murakami, M. Itagaki and S. Oikawa, J. J. Appl. Phys. **46** (2007) 1157

[6] S. Murakami *et al.*, Nucl. Fusion **39** (1999) 1165

[7] K. C. Shaing, Phys. Fluids **27** (1984) 1567

[8] K. Itoh, S. -I. Itoh, A. Fukuyama, H. Sanuki and M. Yagi, Plasma Phys. Control. Fusion **34** (1994) 123